Journal Pre-proof

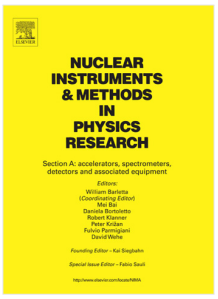

Enhancing neutron detection capabilities of a water Cherenkov detector

Iván Sidelnik, Hernán Asorey, Nicolás Guarin, Mauricio Suaréz Durán, José Lipovetzky, Luis Horacio Arnaldi, Martín Pérez, Miguel Sofo Haro, Mariano Gómez Berisso, Fabricio Alcalde Bessia, Juan Jerónimo Blostein

PII: S0168-9002(19)31477-9
DOI: https://doi.org/10.1016/j.nima.2019.163172
Reference: NIMA 163172

To appear in: *Nuclear Inst. and Methods in Physics Research, A*

Received date : 1 July 2019
Revised date : 18 October 2019
Accepted date : 22 November 2019

Please cite this article as: I. Sidelnik, H. Asorey, N. Guarin et al., Enhancing neutron detection capabilities of a water Cherenkov detector, *Nuclear Inst. and Methods in Physics Research, A* (2019), doi: https://doi.org/10.1016/j.nima.2019.163172.

This is a PDF file of an article that has undergone enhancements after acceptance, such as the addition of a cover page and metadata, and formatting for readability, but it is not yet the definitive version of record. This version will undergo additional copyediting, typesetting and review before it is published in its final form, but we are providing this version to give early visibility of the article. Please note that, during the production process, errors may be discovered which could affect the content, and all legal disclaimers that apply to the journal pertain.

© 2019 Published by Elsevier B.V.

Journal Pre-proof

Enhancing Neutron Detection Capabilities of a Water Cherenkov Detector

Iván Sidelnik[a,b,f,*], Hernán Asorey[b,d,e,f], Nicolás Guarin[b], Mauricio Suaréz Durán[c], José Lipovetzky[a,b,d,f], Luis Horacio Arnaldi[b,d,f], Martín Pérez[b,d,f], Miguel Sofo Haro[a,b,f], Mariano Gómez Berisso[a,b,f], Fabricio Alcalde Bessia[a,b,f], Juan Jerónimo Blostein[a,b,f]

[a] *Consejo Nacional de Investigaciones Científicas y Técnicas (CONICET), Argentina*
[b] *Instituto Balseiro, CNEA-UNCuyo, Argentina*
[c] *Grupo de Investigación Integrar y Departamento de Física y Geología, Universidad de Pamplona, Norte de Santander, Colombia*
[d] *Comisión Nacional de Energía Atómica (CNEA)*
[e] *Escuela de Tecnología y Medio Ambiente, UNRN*
[f] *Centro Atómico Bariloche, Av. Bustillo 9500, S. C. Bariloche, 8400, Argentina*

Abstract

In this work we show the neutron detection capabilities of a water Cherenkov detector (WCD) using pure water, as well as an aqueous solution of sodium chloride as the detection volume. The experiments were performed using a WCD with a single photomultiplier tube (PMT), and a ^{252}Cf neutron source. We show that fast neutrons from a ^{252}Cf source directly impinging the detector can be clearly detected and identified over the natural radiation background. We also present results from numerical simulations that describe the response of the WCD to neutrons of different energies. To do this, a detailed model for the WCD and of the neutron source spectra have been implemented. The implemented simulation code takes into account the interaction processes involved in the detection of neutrons using WCD, and support the experimental evidence introduced in this work. Being both the active volumes analyzed in this work (pure water) and the additive (sodium chloride), cheap, non-toxic and easily accessible materials, the results obtained are of interest for the development of large neutron detectors for different applications. Of particular importance are

*Corresponding author
Email address: sidelnik@cnea.gov.ar (Iván Sidelnik)

October 16, 2019

Journal Pre-proof

the detection of special nuclear materials, as well as those applications related with space weather phenomena. We conclude that WCD used as neutron detectors could be a replace or a complementary tool for standard neutron monitors based on ^{3}He.

Keywords: Neutron detection, Water Cherenkov Detector, Cherenkov effect, Homeland Security, Space Weather

2018 MSC:

1. Introduction

Water Cherenkov detectors (WCD) of large volumes using ultra pure water are sensitive to relativistic charged particles and also to high energy photons. These detectors are used in a variety of implementations, from a diversity of astrophysical studies such as the Pierre Auger Observatory [1] and the Latin American Giant Observatory (LAGO) [2, 3]; to the detection of Special Nuclear Material (SNM) for homeland security [4, 5]. The usage of this kind of detectors is supported by their proven robustness in different field conditions, low costs, large volume and high performance.

In recent years there has been a growing interest in the measurement of neutrons using WCD with different additives to increase sensitivity. The Super Kamiokande collaboration, for example, has been testing different approaches to the use of gadolinium (Gd) in their very large 50,000 ton WCD [6, 7]. The idea behind this work is to tag neutrons produced in water by inverse beta reaction as an indication of the detection of astrophysical anti neutrinos coming from Supernovae.

It is worth noting that, a ground based space weather oriented experiment that, uses neutron monitors to study low energy cosmic ray flux variations can use WCD as an alternative detector. In particular, the LAGO [8], the Pierre Auger Observatory [1] and HAWC [9] collaborations use WCDs to measure changes in the flux of cosmic rays and relate them with solar activity indicators. These detectors span over total water detection volumes from $\sim 1\,\mathrm{m}^3$ to $\sim$

Journal Pre-proof

$20000\,\mathrm{m}^3$. There are studies that found that the major change in low energy cosmic rays are produced by neutrons as a part of secondary showers produced by cosmic ray particles [8, 10]. Corsika simulations performed by the LAGO Collaboration shows that for cosmic rays that has its primary energy in the $10^{11}\,\mathrm{eV}$ to $10^{15}\,\mathrm{eV}$ range, and for different altitudes[1], the flux of secondaries is dominated by high energy neutrons at ground level [8, 10].

Non proliferation and homeland security are other possible uses of this type of inexpensive water-based detectors. Fissile elements as uranium or plutonium produce simultaneous emissions of multiple neutrons. In this field, it is worth to notice that ^{3}He-based neutron detectors have had a growing application for homeland security. This is so because the ^{3}He-based ionization tubes are non-cryogenic, safe, non corrosive, highly efficient for thermal neutron detection, and have a low gamma sensitivity. The ^{3}He-based neutron detectors, in combination with moderator materials, are efficient for the detection of fast neutrons emitted from nuclear fission. However, for this reason, the homeland security application of ^{3}He detectors has triggered a crisis in the ^{3}He supply and its price is significantly increasing [11]. Therefore, neutron detectors of large solid angle, inexpensive materials with good noise rejection are desirable. In this context, WCDs employing different materials [12, 13], as well as other detection techniques have been implemented [14, 15, 16, 17, 18, 19, 20].

In this work we analyze the response for neutron detection of a WCD using as active volume pure light water, and a novel approach using aqueous solutions doped with NaCl testing different concentrations.

It must be noted that the work [21] aimed to detect neutrinos uses heavy water (D_2O), doped with NaCl while our work employees light water. In SNO the deuterium is present mainly for the conversion of neutrinos in to neutrons, this element is crucial for the neutral current interaction used to capture neutrinos coming from the sun. This is not the case of the detection system that

[1] [10] shows simulations for a site at La Serena, Chile 28 m a.s.l and at Chacaltaya, Bolivia, 5240 m a.s.l.

Journal Pre-proof

we have implemented. Also, since the case of study of SNO is the neutrino detection, and the aim of this work is the neutron detection, the active volume involved in SNO is one thousand times larger than that of the neutron detector introduced here. In addition, the neutron production in the SNO detector is homogeneously distributed in to the liquid, while in our detector the neutron arrives from outside sources.

The outline of the article is as follows: Sec. 2.1 describes the detection technique implemented in this work. In Sec. 2.2 we discuss the reasons for the choice of NaCl as additive to the pure water in order to enhance the neutron detection. Sec. 2.3 shows details on the ^{252}Cf source used and the shielding. Sec. 2.4 introduces a simulation scheme implemented in Geant 4 to detailed describe the WCD implemented in this work. Sec. 3 shows the experimental results as well as the simulations. A comparison of the measurements performed with the simulation using Geant 4 is showed in Sec. 4. And finally, the conclusions and future perspectives of WCD in the field of neutron detection are presented in Sec. 5.

2. The WCD detection technique

2.1. The detector

Charged particles moving faster than the speed of light in the medium produce Cherenkov photons when $\beta \geq 1/n$, where $n(>1)$ is the refractive index of the medium, and $\beta = v/c$ the velocity of the particle in units of the speed of light. If the medium is not opaque, the Cherenkov light can be detected by placing a light detector into it. Besides, if the charged particle is ultra-relativistic, i.e. $\beta \approx 1$, the angle of the Cherenkov cone has a constant and maximum value. In water, this angle is $\alpha_{Ch} = 41.4°$, with respect to the incident particle speed direction. Water is widely used as a detector material because it is clear, non toxic, inexpensive and can be used in very large volumes. With index of refraction n_{H_2O} =1.33, the Cherenkov energy threshold for electrons is E^e_{Ch}∼775 keV; for muons the threshold is 160 MeV and for protons it is 1400 MeV. For photons,

Journal Pre-proof

the Cherenkov threshold for pair production is $E_\gamma > 2E^e_{ch} \simeq 1.6\,\mathrm{MeV}$, greater than the well known threshold for the pair creation process.

The WCD installed in the Neutron Physics Department Laboratory at Centro Atómico Bariloche, Argentina, is an autonomous, reliable, simple and inexpensive detector. We have built two versions one of $0.5\,\mathrm{m}^3$ and other of a $1.0\,\mathrm{m}^3$, they consist of a stainless steel commercial water tank of cylindrical shape, with 96 cm of diameter and different heights. Both detectors have 8" Hamamatsu R5912 PMTs, plus a digitizer board of custom design used by the LAGO Collaboration [22]. The detector is controlled by a Nexys II FPGA with an overall power consumption of less than 8 W. In Fig. 1, there is an scheme of the experimental set up, showing the detector characteristics as well as the shielding and source disposition. The simulations were performed with neutron from a ^{252}Cf source impinging at the middle of the height of the detector. In the experiment the source was placed also at the middle of the height of the detector.

The detectors also have a 0.12 mm thick inner coating of Tyvek®, a diffusive and reflective fabric. The spectral-directional reflectivity of Tyvek® and the uses for this kind of detection systems were studied at [23].

The 8" Hamamatsu R5912 PMT has a spectral response spanning from 300 nm to 650 nm with a peak at about 420 nm [24], that matches the well known Cherenkov light spectrum produced in water, which is continuously extended in the range of 300 nm to 600 nm, approximately [25, 26, 27, 28].

The stainless steel container is light tight and holds the aqueous solution of H_2O plus different concentrations of NaCl.

A detailed study of muon tracks in this kind of WCD [29] shows that water is almost transparent to the Cherenkov light. Taken this in to account, it is expected that the signal intensity observed after the neutron absorption will be almost independent of the impinging zone [29]. The information about the entry point of neutrons, or its direction is lost. When a neutron enters the active volume it is randomly scattered and thus moderated. After the moderation, the absorption of the neutron produces prompt gammas that are isotropically

Journal Pre-proof

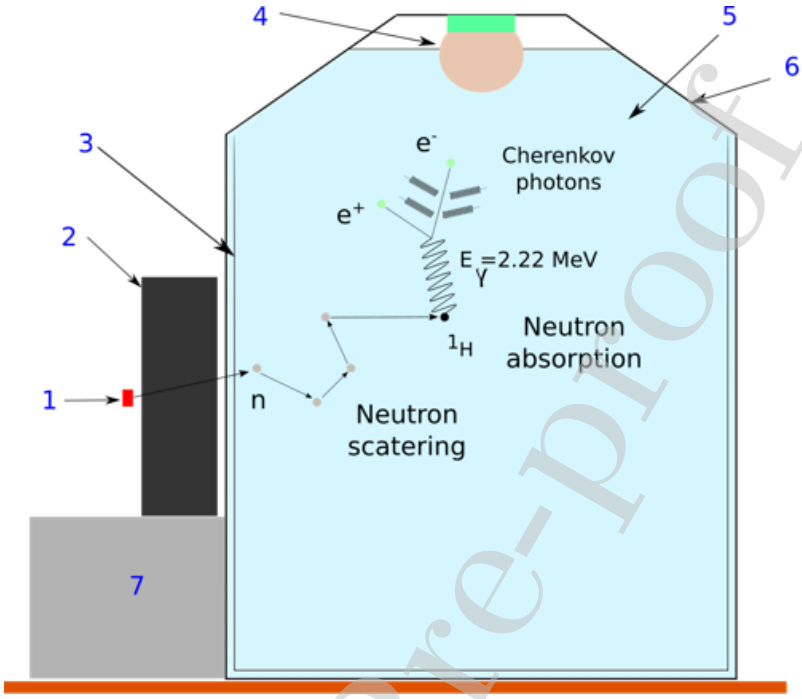

Figure 1: Scheme view of the water Cherenkov detector experimental set up. 1 - neutron source placed at the middle of the height of the detector. 2 - lead shielding, to reduce the gamma contribution. 3 - Tyvek inner coating. 4 - 8" Hamamatsu R5912 PMT. 5 - active volume, aqueous solution. 6 - stainless steel container. 7 - concrete block to to increase the source plus shielding height and shield the gammas from the source to go in to the ground.

emitted. These gammas produce electrons mainly via Compton scattering, and therefore the direction of the incident gamma is loosed. Then the Cherenkov photon emission is isotropic and the reflectivity of Tyvek has the effect of loose the direction of the Cherenkov cones. For these reasons this detector do not provide information about the entry point or direction of the incident neutron.

2.2. The additive

After the firsts studies [12], that showed positive results about neutron detection using a water Cherenkov detector with pure water and only one PMT attached to the liquid, it was concluded that an enhancement on the neutron signal intensity to stand out over the other particle background was required.

Journal Pre-proof

The signal to noise ratio could be enhanced by the addition of an element that absorbs neutrons emitting high energetic particles that produces a Cherenkov signal of higher intensity.

Since the abundance of the ^{35}Cl isotope is $\sim$75% and the isotopic cross section is 43.84$\pm$0.17 b [30], we chose to use NaCl, a compound that can be easily dissolved in water, does not significantly attenuate the Cherenkov light, does not posses serious contamination risks to the environment if spilled, and can serve as a preservative for the water.

In Fig. 2 it is shown a comparison of the gamma prompts lines emitted from ^{35}Cl(n,γ)^{36}Cl reaction, that spans from a 292 keV to more than 8500 keV in energy, in blue thin lines [31] and the 2223 keV line from the ^{1}H in red thick line. The intensity of the lines are referred to the 2223 keV line, according to [31]. These are the decay gamma rays from thermal neutron capture, plotted as a function of their energy against the absorption cross section for gamma production.

It is also displayed the Cherenkov threshold (E^e_{Ch})for electrons in water with a refraction index n$\simeq$1.33, that is $\sim$775 keV, in yellow arrow, and the threshold in NaCl, with n$\simeq$1.54 ([32]) that is 672 keV in green arrow. Since an aqueous solution resulting in add NaCl to H_2O will have an intermediate value of n, we show this two values and the corresponding E^e_{Ch} as a reference.

From Fig. 2 it is clear that the prompt gamma lines emitted after the neutron absorption by the isotope ^{35}Cl are larger in number and has 74 more energetic gamma rays than the 2223 keV emission of the ^{1}H. This would result in an increase of Cherenkov signal because the Cherenkov photon emission is directly proportional to the energy of the charged particles, and gammas of 8578.6 keV (with all the others of lower energy in cascade) will produced more energetic electrons than gammas of 2223 keV.

Performing a rough estimation, being $\sigma_{^1H}$=0.332 b and $\sigma_{^{35}Cl}$=43.84 b, the neutron absorption cross sections, we take as a reference for the amount of mass of NaCl that diluted in H_2O equals the absorption rates in ^{35}Cl and ^{1}H. In 1 m^3 of water this condition is fulfilled whit a dilution of $\sim$52 kg of NaCl. This

Journal Pre-proof

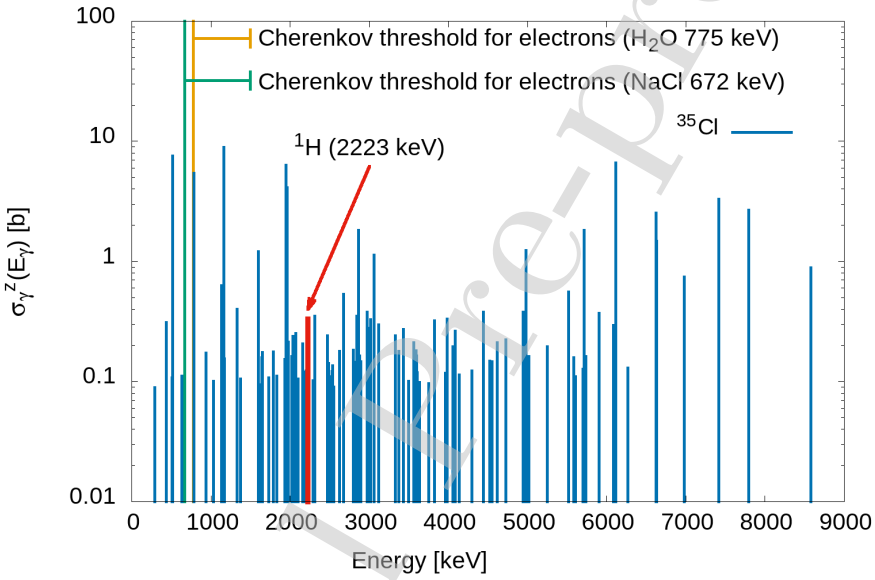

Figure 2: Intensities of the gamma prompt lines from the ^{35}Cl(n,γ)^{36}Cl reaction (blue thin lines) compared with that of 2223 keV line form the of ^{1}H(n,γ)^{2}H (in red thick line) from [31]. It is also showed the Cherenkov threshold in H_2O for electrons that is 775 keV, in yellow arrow and the threshold in NaCl 672 keV, in green arrow.

Journal Pre-proof

Journal Pre-proof

motivated us to perform simulations and experiments with pure H_2O, and with the addition of different amounts of industrial NaCl into the water.

There is a notable difference in the physics of the detector introduced in this work and the detector of SNO used for neutrinos [21]. The neutron absorption cross section of D is significatively smaller than that of H. For this reason in SNO the intensity of the D prompt gamma lines are negligible with respect of that of H. When D_2O is employed the prompt gamma lines are mostly emitted by Cl, while when H_2O is employed the prompt gammas are emitted from Cl as well as from H. Therefore, it should be expected that the signal of the WCD doped with NaCl will be more clear for the D_2O case. Nevertheless, in this work we will show that even using H_2O the neutron detection is possible. The addition of NaCl to H_2O generates a stronger signal from neutrons than that coming from the H alone.

2.3. ^{252}Cf neutron source used and shielding

A ^{252}Cf neutron source, with a flux of 1.90×10^4 neutrons per second (isotropically emitted) was used. ^{252}Cf emits neutrons through spontaneous fission with an energy spectrum that spans from 0.003 up to $\simeq$15 MeV [35, 36]. We performed measurements with lead shielding, to diminish the effect of the gamma photons emitted by the Cf source, leaving mainly fast neutrons entering the detector. Fig. 3 shows the gamma spectrum of a Cf source in dashed line, from data of ref. [33], and in continuous line the attenuated spectrum by using a 10 cm lead shield between the source and the detector. This shows how we avoid most of the gammas coming from the source to enter into the detector, leaving mainly fast neutrons emitted by the source.

2.4. Geant 4 simulation scheme

We performed a detailed simulation of the implemented device experimental set-up, taking in to account the physical interactions and particles produced into the detector using the Geant 4 code [37]. The detector is a 96 cm diameter by 133 cm tall and 0.5 mm thick stainless steel cylinder, which is full of water,

Journal Pre-proof

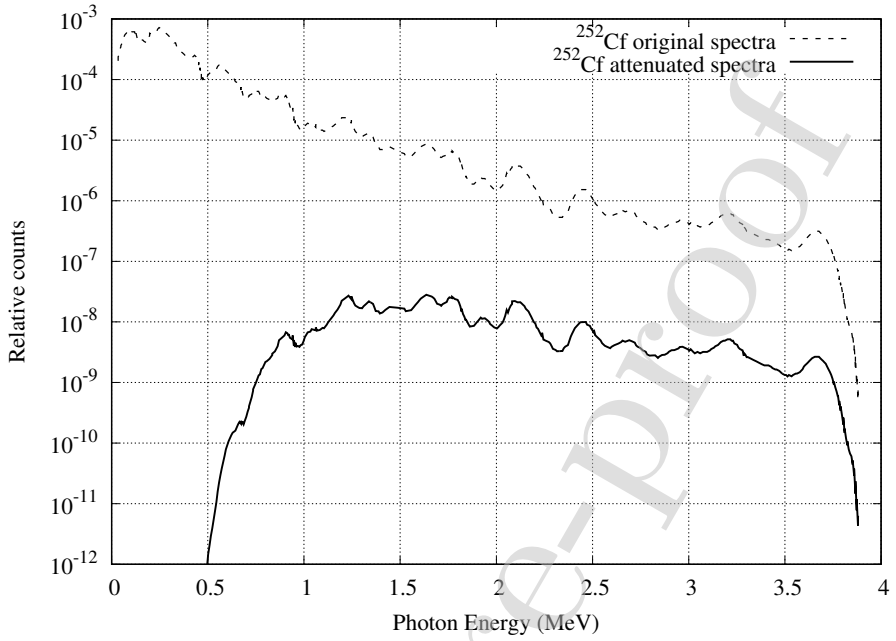

Figure 3: Gamma spectrum emitted by a ^{252}Cf source taken from reference [33], in dashed line and the attenuated spectrum by the 10 cm lead shield in continuous line [34].

or with water plus the additive. There is also an hemisphere of 5 cm tall and 10.16 cm of radii that simulates the PMT photocathod and it is located at the top of detector. Between the water and the stainless steel volume there is a thin layer (with approximately 0.12 mm of thickness) that has the reflective and refractive properties of Tyvek®. For the simulation it was also used the quantum efficiency (QE) reported by Hamamatsu for the R5912 PMT to sort the acceptance or rejection of a Cherenkov photon in to the PMT [24].

The simulations were performed using the spectral shape of fast neutrons from a ^{252}Cf source [38], a fission spectrum. As active volume we used pure water (H_2O) and water with different additive (NaCl) concentrations, 2.5%, 5% and 10%, in mass (see Section 2.2).

Journal Pre-proof

Journal Pre-proof

3. Results and discussion

3.1. Experimental results using a ^{252}Cf neutron source

For each experimental configuration, the implemented electronics records the spectrum of the registered pulses. The ADCq magnitude (horizontal axis of the spectra) represent the charge of each recorded event. In Fig. 4 we show the experimental results from the measurements obtained with the ^{252}Cf neutron source, in which the contribution of the background has been subtracted [22]. The measurements were made in 300 s and the subtracted background was measured immediately before the source measurements. Measurements using pure water and water with 2.5% in mass of NaCl are showed in red circles and in green squares respectively. The units of charge of the recorded events are ADC_q, i.e., the integral of a single, 300 ns-long pulse as a function of time (measured in time intervals of 25 ns) after the subtraction of the signal baseline. It is clear from the Fig. that the signal using the additive results more intense than the one with pure water.

In Section 4 we show an analysis of this measured spectra compared to the Monte Carlo simulations performed with Geant 4 code.

3.2. Simulation results using Geant 4

Simulations in Geant 4 were performed including all the relevant parameters of the detector (Section 2.4). First we aimed to understand the absorption process of the neutrons, comparing pure H_2O and including the NaCl in different proportions. In Table 1 we show the number of neutron captures within the active volume in the case of H_2O and with the additive. We calculate the absorption in ^{1}H, in ^{35}Cl and the total number. The simulations shows an increase in the number of captures when the NaCl is added to the H_2O. It is worth to note that for 5% of NaCl content in water the captures in H and Cl are essentially balanced, as our firsts rough estimation showed in Section 2.2. It is also worth noting that for the 10% of NaCl added the absorption numbers are reversed and the Cl absorbs almost twice than the H. It can be said that

Journal Pre-proof

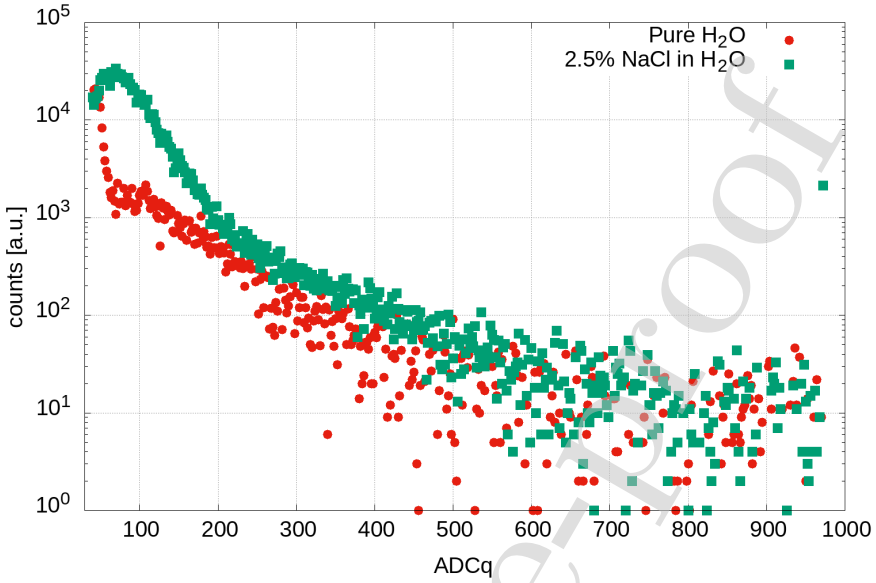

Figure 4: Spectra of the experiments using a ^{252}Cf neutron source, after background subtraction. The red circles shows measurements with pure water and green squares using water with 2.5% in mass of NaCl. The addition of NaCl show an increase in the signal resulting in a huge difference with respect to the pure water.

the total number of neutrons captured are increased with the addition of NaCl, but does not have a large variation when the amount is increased from 2.5% to 10%.

Sensitive volume	Captures (^{252}Cf)			Max. absorption
	^{1}H [%]	^{35}Cl [%]	Total [%]	distance [cm]
H_2O	4.8	0	4.8	10.2
H_2O + 2.5% NaCl	7.3	3.7	11.3	9.7
H_2O + 5% NaCl	5.7	5.5	11.6	9.8
H_2O + 10% NaCl	4.1	7.5	12.3	9.5

Table 1: Captures in ^{1}H, in ^{35}Cl, the total number of neutron absorbed and the distance of maximum absorptions from simulations, using the simulated spectrum of a ^{252}Cf neutron source.

Fig. 5 shows the distance from the edge of the detector facing either the ^{252}Cf

Journal Pre-proof

neutron source and the absorption point. The maximum absorption observed is at (10.2±0.1) cm for the pure water case (red circles) and (9.6±0.1) cm for the addition of NaCl (green squares for 2.5%, violet triangles up for 5% and yellow triangles down for 10% in mass). It is clear that the number of absorptions results higher with the addition of NaCl, this material increases the neutron absorption (and therefore the neutron detection efficiency) without affecting significantly the moderation process in water. It is worth to remembering that both neutron absorption reactions (in water and in NaCl) follow the well known $1/v$ law [39], and therefore the moderation process becomes necessary before the neutron absorption.

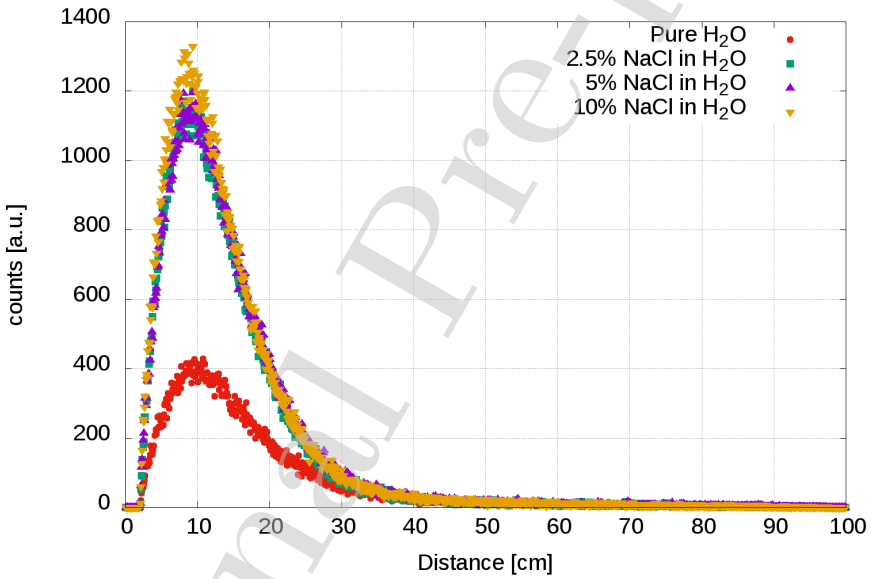

Figure 5: Capture distance of neutrons in pure water and water with additive. Top: simulations using a ^{252}Cf source. The distance with the most captures from the border of the detector (∼10 cm) for water (red circles) and (∼9.6 cm) for water with every concentration of NaCl employed as an additive. The number of captures results larger due to the higher σ_{abs} of the ^{35}Cl.

The different intensities observed in Fig. 5 are due to the fact that once reached the thermal equilibrium with the material, the thermal neutron leak

Journal Pre-proof

becomes less probable as the effective cross section increases [30]. The quasi-saturation observed at the maximum is due to the fact that (however large its absorption cross section is) it is impossible for the system to absorb more thermal neutrons that the ones that managed to thermalize.

Fig. 6 shows the gamma particles generated in the active volume of the detector after the neutron absorption, as a function of the energy. In the top figure we take in to account the pure water situation (red line full circle) and the different concentrations of NaCl, 2.5% (green squares), in the bottom Fig. 5% (empty purple triangles up) and 10% (full yellow triangles down), using the spectrum of a ^{252}Cf source. Fig. 7 shows in cumulative intensity of the prompt gamma particles emitted in Fig. 6 from the highest energy generated in the active volume of the detector after the neutron absorption. With the pure water situation (red circles) and the different concentrations of NaCl, 2.5% (green squares), 5% (purple triangles up) and 10% (yellow triangles down), in all cases we use the spectrum of a ^{252}Cf source. The gammas emitted from pure H_2O, show the most prominent signal at 2223 keV, as expected, with the addition of prompt gammas emitted from other interactions. In the case of the additive incorporated to the water, more energetic gammas are emitted mainly due to neutrons absorption in ^{35}Cl, thus increasing the intensity of the pulse that constitute the signal. As an important feature it can be seen that, for the concentrations considered in this work the 2223 keV line is still important even when the NaCl is added, but the contribution to the cumulative intensity due to the 2223 keV gammas are reduced as the additive concentration increase because the more ^{35}Cl is present the less ^{1}H absorbs neutrons. This can also be appreciated in the other lines, that have a greater contribution as the NaCl concentration is higher. It is also worth notice that the gamma production extends towards more than 8 MeV, where the last line of ^{35}Cl gamma prompt is.

Fig. 8 shows the electrons emitted inside the active volume of the detector by the gamma particles showed in Fig. 6 and 7. The Compton edge can be clearly distinguished for the electrons produced in pure water by the 2223 keV

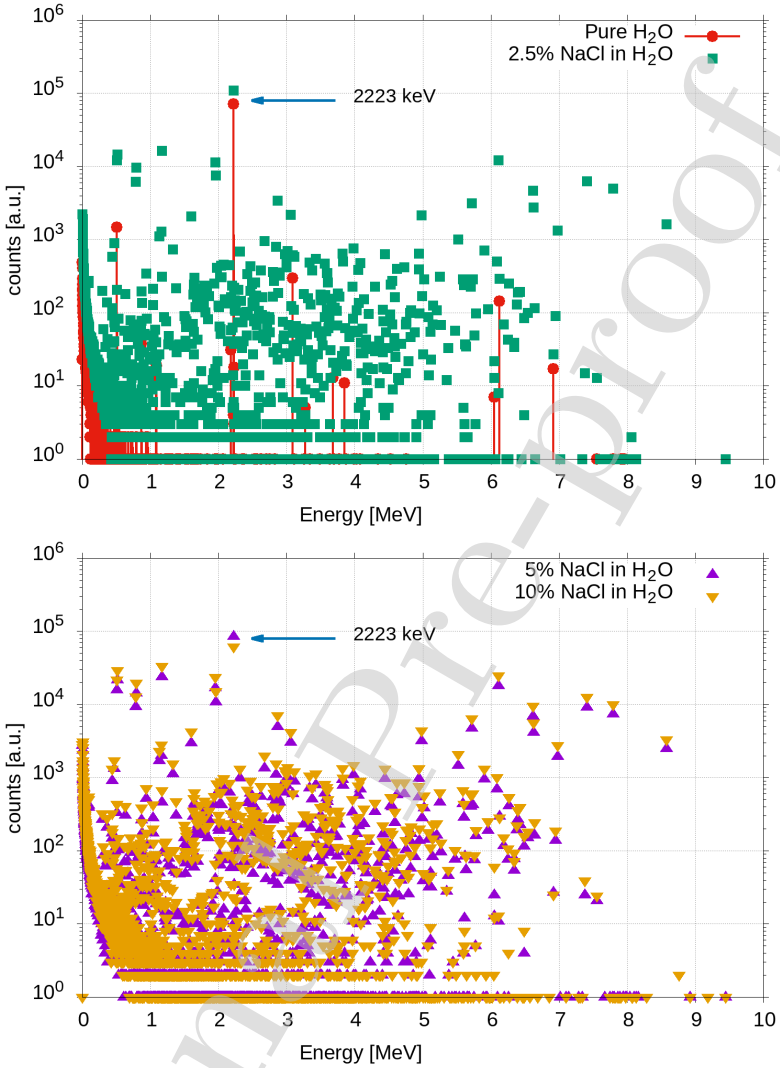

Figure 6: Gamma particles produced in the simulation using the spectra of a ^{252}Cf source. Top: pure water situation (red line full circle) and 2.5% of NaCl (green squares). Bottom: 5% (empty purple triangles up) and 10% (full yellow triangles down). The 2223 keV peak can be noted in all cases as well as that of high energy gammas lines emitted after the neutron absorption in ^{35}Cl when the NaCl is present.

Journal Pre-proof

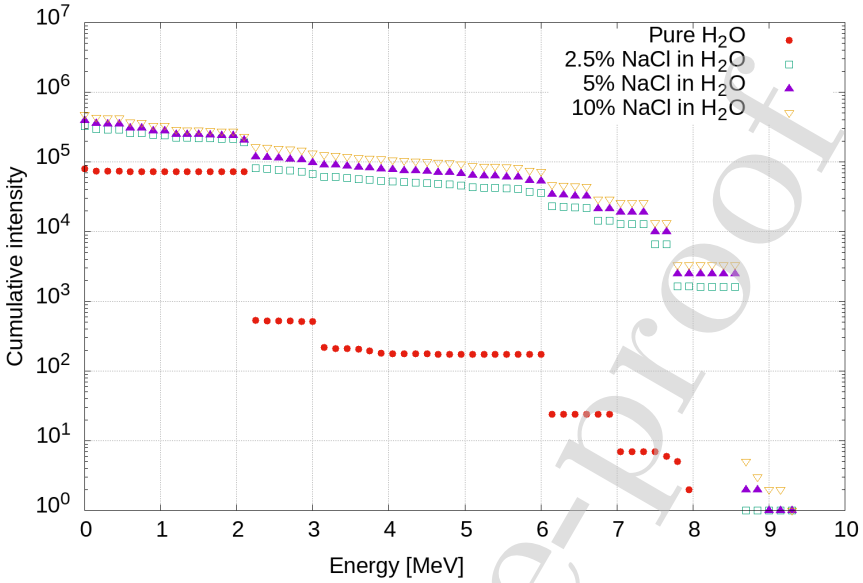

Figure 7: Cumulative intensity of the gamma lines presented in Fig. 6 which have been obtained from the simulation using the spectra of a ^{252}Cf source with pure water situation (red circles) and the different concentrations of NaCl, 2.5% (green squares), 5% (purple triangles up) and 10% (yellow triangles down).

gamma line (red line). For this energy, the most energetic electron produced by Compton interaction has E_{elec} ≃1994 keV. For the water with different additive concentrations the Compton edge starts at E_{elec} ≃8330 keV. This is the maximum energy that an electron can have after a Compton interaction with a 8578.6 keV gamma photon, being the latest the maximum energy emitted after a neutron absorption in ^{35}Cl. For gammas energies higher than 2223 keV, a mix of electron Compton edges at energy higher than that formerly mentioned, increases the contribution of energetic electrons into the detector active volume, which would result in an increase of the Cherenkov signal.

In Fig. 9 it can be appreciated the Cherenkov photons production by the electrons showed in Fig. 8. As the refraction index of the active volume changes with the addition of NaCl, see Section 2.2, there will be a larger production

Journal Pre-proof

Journal Pre-proof

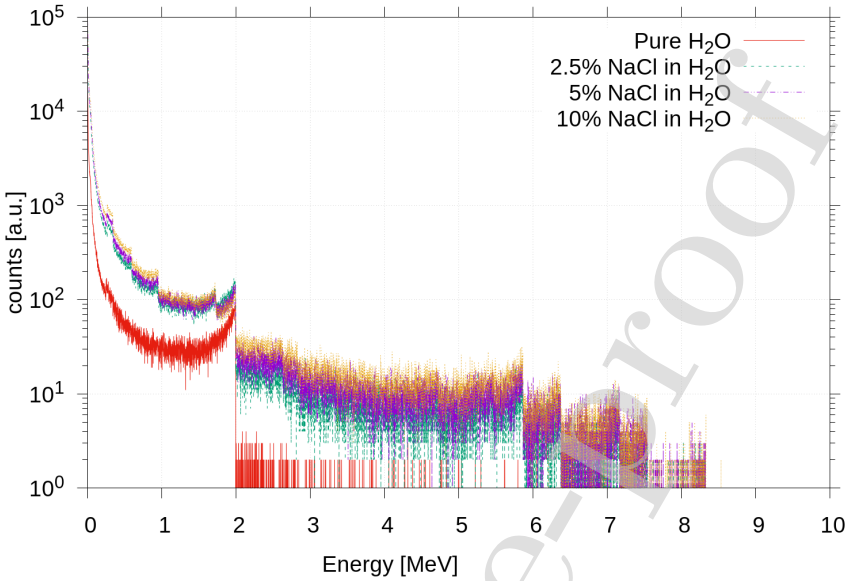

Figure 8: Electron spectra produced inside the detector by the interaction of gammas within the active volume (Fig. 6), which are produced mostly by Compton interaction. Simulations were performed using a ^{252}Cf neutron source.

of Cherenkov photons by less energetic electrons as the amount of additive increases. This gives an increase of the low number of photons region for the NaCl situation with respect to the pure water, that can be appreciated in Fig. 9 under ∼20 photons. In this part of the plot, can also be appreciated the relation between the peaks for different NaCl concentrations. The absorption of visible photons by ^{35}Cl could have the effect of decrease the number of Cherenkov photons as can be seen in Fig. 9, showing that when more ^{35}Cl is present the peak of Cherenkov photons decrease.

For number of photons greater than 20, it can be appreciated the increase in the number for the NaCl situation, this time due to the emission of gammas with more than 8 MeV, showing that the more ^{35}Cl is present more Cherenkov photons are, leaving more signal into the detector.

One important characteristic of the simulations is that not only the sig-

Journal Pre-proof

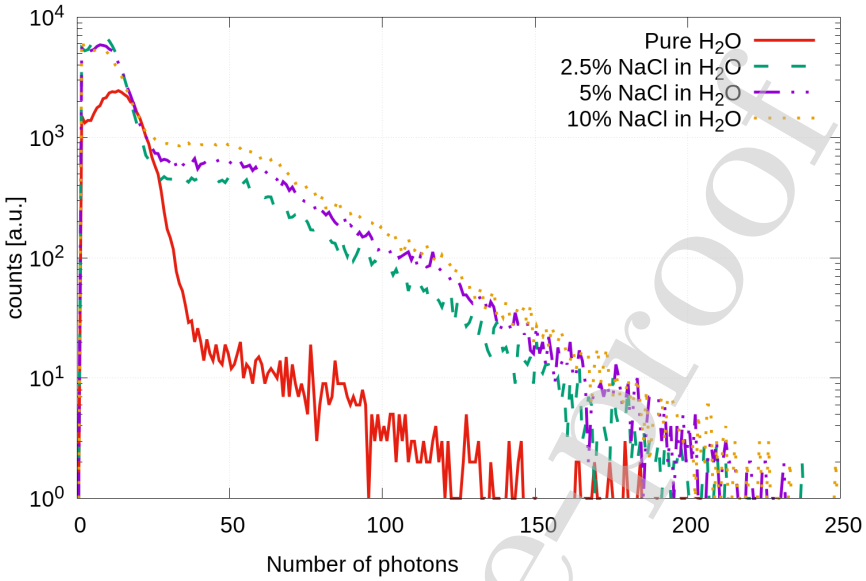

Figure 9: Number of Cherenkov photons recorded in total, produced by the electrons spectra showed in Fig. 8 inside the active volume of the detector.

nal results enhanced when NaCl is added to H_2O (producing more energetic electrons) having a positive impact in this neutron detection technique, also increasing the detection efficiency. We observed that the addition of 2.5% of NaCl produces a significantly improvement in the response of the detector, similar to that obtained at higher NaCl concentrations.

4. Data and simulation comparison

The number of Cherenkov photons as presented in Fig. 9 should be proportional to the pulse charge of an event measured in ADCq units. In order to compare the simulations with the experimental results, for the pure water case we rescaled the calculated spectrum, multiplying by a factor of (1.56±0.03) the number of photons and by (118±12) the count number. These factors were obtained by fitting the Geant 4 simulations to the experimental results in the 45-150 ADCq range. This match is showed in Fig. 10. Below 45 ADCq the

Journal Pre-proof

effect of the applied electronic threshold produces a declination of the measured spectrum. For this reason events under this value were not taken in to account. Above 150 ADCq there is an effect where the measured spectrum goes over the simulated one, this higher energetic signals could be produced by the impurities of the tap water employed that makes it emit high energy gammas and also some impurities that could interact with the neutrons coming from the source that gives high energy signals. It must be noted that in this range the spectra shows a notable change in its slope observed at 65 ADCq. For ADCq lower than 65 the dominant emission is the 2223 keV, while for higher ADCq values the signal is dominated by the prompt gamma emissions from oxygen.

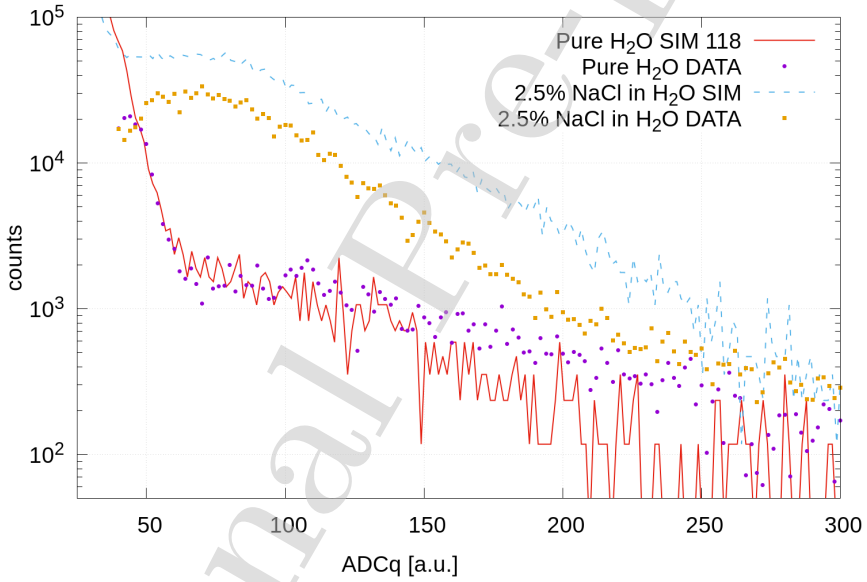

Figure 10: Analysis of the spectra of Cherenkov photons (from Fig. 9) simulated with Geant 4 normalized to match the experimental spectra of neutrons detected with the WCD (from Fig. 4), including pure water and aqueous solution with 2.5% of NaCl. For further details see text.

As for the spectra with 2.5% of NaCl in the aqueous solution, using the same rescaling obtained with the pure water there is a shifting in the measured spectrum with respect to the simulation. This shift could be due to impurities

Journal Pre-proof

from the added NaCl that could produced Cherenkov light absorption resulting in a reduction of the signal.

5. Conclusions

The main conclusion of this work is that the use of NaCl as dopant produce a remarkable enhancement in the neutron detection capabilities of a WCD. An experimental set up, and a Geant 4 model were implemented, which allows to describe the physics of the detector.

Our previous work [12, 13] shows that a WCD with pure water and a single PMT is possible. The addition of NaCl clearly enhances the capabilities of neutron detection in the Cf source energy range (up to $\sim$15 MeV). The characteristics of ^{35}Cl and its interaction with neutrons are shown in Section 2.2.

The results in Section 3.2 show that, using different amounts of NaCl in mass inside the active volume of the detector composed mostly by H_2O has a clear impact in the neutron captures by the aqueous solution. This is followed by an emission of more energetic gamma particles that results in a increase of the electron production finishing in a higher Cherenkov signal as expected from our preliminary analysis of the additive. In this direction the experimental results presented in Section 3.1 show a clear improvement of the spectra (with background subtracted) of measurements performed using different amounts con NaCl in the water. The simplicity of the detector allows us to incorporate the necessary amount of additive to the active volume in a way we can gain detection efficiency.

It is worth to notice that the neutron detector introduced in this work presents several advantages over previously used water Cherenkov detectors for neutron detection [4, 5, 40, 41]. The main advantages are that the active volume of the detector employed in this work is simply pure water (an inexpensive material, abundant, and no contaminant) using NaCl as an additive. NaCl does not present high contamination risks, and conserves the liquid free of bacteria. Moreover, due to the use of only one PMT, the electronics of the neutron

Journal Pre-proof

detector introduced in this work are cheaper and simpler than that of the previous neutron WCDs formerly mentioned which use several PMTs coupled to the active volume.

Finally the obtained results in this work are of interest for the development of low cost neutron detectors with large active volumes for different applications. Of special importance are those related with space weather phenomena as well as those for for non proliferation enforcement and for "Special Nuclear Material" (SNM) detection for homeland security. We conclude that WCD with NaCl as additive can be used as a replace or a complementary tool for standard neutron monitors based on ^{3}He.

Acknowledgment

The authors would like to acknowledge the full support by CONICET and CNEA. We are very thankful to the technicians in our lab that help to set up the detectors: P. D'avanzo, A. Mansilla, F. Y. Moreira, G. Anibal. This work has been done thanks to the following grants: PICT ANPCyT 2015-1644, PICT ANPCyT 2016-2096, PIP CONICET 2011 0552, UNCuyo Proy. Cod. 06/C483 and Cod. 06/C594.

References

[1] The Pierre Auger Cosmic Ray Observatory, Nuclear Instruments and Methods in Physics Research Section A: Accelerators, Spectrometers, Detectors and Associated Equipment 798 (2015) 172 – 213. doi:https://doi.org/10.1016/j.nima.2015.06.058.

[2] The LAGO Collaboration, The LAGO Project (2019).
URL http://lagoproject.net/

[3] M. Suárez-Durán, H. Asorey, S. Dasso, L. Núñez, Y. Peréz, C. Sarmiento, The LAGO Space Weather Program: Directional Geomagnetic Effects,

Journal Pre-proof

Background Fluence Calculations and Multi-Spectral Data Analysis (2016) 34–41doi:10.22323/1.236.0142.

[4] S. Dazeley, M. Sweany, A. Bernstein, SNM detection with an optimized water Cherenkov neutron detector, Nuclear Instruments and Methods in Physics Research Section A: Accelerators, Spectrometers, Detectors and Associated Equipment 693 (2012) 148 – 153. doi:https://doi.org/10.1016/j.nima.2012.07.026.

[5] M. Sweany, A. Bernstein, N. Bowden, S. Dazeley, G. Keefer, R. Svoboda, M. Tripathi, Large-scale gadolinium-doped water Cherenkov detector for nonproliferation, Nuclear Instruments and Methods in Physics Research Section A: Accelerators, Spectrometers, Detectors and Associated Equipment 654 (1) (2011) 377 – 382. doi:https://doi.org/10.1016/j.nima.2011.06.049.

[6] T. Mori, Status of the Super-Kamiokande gadolinium project, Nuclear Instruments and Methods in Physics Research A 732 (2013) 316–319. doi:10.1016/j.nima.2013.06.074.

[7] H. Watanabe, H. Zhang, K. Abe, et al, First study of neutron tagging with a water Cherenkov detector, Astroparticle Physics 31 (4) (2009) 320 – 328. doi:https://doi.org/10.1016/j.astropartphys.2009.03.002.

[8] H. Asorey, L. A. Núñez, M. Suárez-Durán, Preliminary results from the latin american giant observatory space weather simulation chain, Space Weather 16 (5) (2018) 461–475. doi:10.1002/2017SW001774.

[9] V. Joshi, A. Jardin-Blicq, HAWC High Energy Upgrade with a Sparse Outrigger Array, PoS ICRC2017 (2018) 806, [35,806(2017)]. arXiv:1708.04032, doi:10.22323/1.301.0806.

[10] R. Calderón-Ardila, A. Jaimes-Motta, J. Peña-Rodríguez, C. Sarmiento-Cano, M. Suárez-Durán, A. Vásquez-Ramírez, for the LAGO Collaboration, Modeling the LAGOs detectors response to secondary particles at

Journal Pre-proof

ground level from the Antarctic to Mexico, PoS ICRC2019.
URL https://pos.sissa.it/358/412/pdf

[11] F. Sachetti, N. Colonna, R. Faccini, B. Guerard, R. Hall-Wilton, F. Murtas, C. Petrillo, A. Pietropaolo, N. Rhodes, L. Quintieri, M. Tardocchi, P. Valente, ^{3}He-free neutron detector and their application, Tech. rep. (2015). doi:10.1140/epjp/i2015-15053-1.
URL https://link.springer.com/article/10.1140/epjp/i2015-15053-1

[12] I. Sidelnik, H. Asorey, J. J. Blostein, M. Gómez Berisso, Neutron detection using a water Cherenkov detector with pure water and a single PMT, Nuclear Instruments and Methods in Physics Research Section A: Accelerators, Spectrometers, Detectors and Associated Equipment 876 (2017) 153 – 155, The 9th international workshop on Ring Imaging Cherenkov Detectors (RICH2016). doi:https://doi.org/10.1016/j.nima.2017.02.048.

[13] I. Sidelnik, H. Asorey, N. Guarin, M. S. Durán, F. A. Bessia, L. H. Arnaldi, M. Gómez Berisso, J. Lipovetzky, M. Pérez, M. Sofo Haro, J. J. Blostein, Neutron detection capabilities of Water Cherenkov Detectors, Nuclear Instruments and Methods in Physics Research Section A: Accelerators, Spectrometers, Detectors and Associated Equipment The 10th international workshop on Ring Imaging Cherenkov Detectors (RICH2018). doi:https://doi.org/10.1016/j.nima.2019.03.017.

[14] T. Gozani, The role of neutron based inspection techniques in the post 9/11/01 era, Nuclear Instruments and Methods in Physics Research Section B: Beam Interactions with Materials and Atoms 213 (2004) 460 – 463, 5th Topical Meeting on Industrial Radiation and Radioisotope Measurement Applications. doi:https://doi.org/10.1016/S0168-583X(03)01590-8.

[15] G. Vourvopoulos, P. Womble, Pulsed fast/thermal neutron analysis: a technique for explosives detection, Talanta 54 (3) (2001) 459 – 468. doi:https://doi.org/10.1016/S0039-9140(00)00544-0.

Journal Pre-proof

[16] J. L. Jones, D. R. Norman, K. J. Haskell, J. W. Sterbentz, W. Y. Yoon, S. M. Watson, J. T. Johnson, J. M. Zabriskie, B. D. Bennett, R. W. Watson, C. E. Moss, J. F. Harmon, Detection of shielded nuclear material in a cargo container, Nuclear Instruments and Methods in Physics Research Section A: Accelerators, Spectrometers, Detectors and Associated Equipment 562 (2) (2006) 1085 – 1088, proceedings of the 7th International Conference on Accelerator Applications. doi:https://doi.org/10.1016/j.nima.2006.02.101.

[17] B. J. Micklich, D. L. Smith, T. N. Massey, D. Ingram, A. Fessler, Figaro: Detecting nuclear material using high-energy gamma rays from oxygen, AIP Conference Proceedings 576 (1) (2001) 1053–1056. doi:10.1063/1.1395486.

[18] P. Kerr, M. Rowland, D. Dietrich, W. Stoeffl, B. Wheeler, L. Nakae, D. Howard, C. Hagmann, J. Newby, R. Porter, Active detection of small quantities of shielded highly-enriched uranium using low-dose 60-kev neutron interrogation, Nuclear Instruments and Methods in Physics Research Section B: Beam Interactions with Materials and Atoms 261 (1) (2007) 347 – 350, the Application of Accelerators in Research and Industry. doi:https://doi.org/10.1016/j.nimb.2007.04.190.

[19] J. Hall, S. Asztalos, P. Biltoft, J. Church, M.-A. Descalle, T. Luu, D. Manatt, G. Mauger, E. Norman, D. Petersen, J. Pruet, S. Prussin, D. Slaughter, The Nuclear Car Wash: Neutron interrogation of cargo containers to detect hidden SNM., Nuclear Instruments and Methods in Physics Research Section B, Beam Interactions with Materials and Atoms 260 (2007) 337–340. doi:101016/jnimb200704263.

[20] K. A. Jordan, T. Gozani, Pulsed neutron differential die away analysis for detection of nuclear materials, Nuclear Instruments and Methods in Physics Research B 261 (2007) 365–368. doi:10.1016/j.nimb.2007.04.294.

[21] B. Aharmim, S. N. Ahmed, et al, Electron energy spectra, fluxes, and

Journal Pre-proof

day-night asymmetries of ^{8}b solar neutrinos from measurements with nacl dissolved in the heavy-water detector at the sudbury neutrino observatory, Phys. Rev. C 72 (2005) 055502. doi:10.1103/PhysRevC.72.055502.
URL https://link.aps.org/doi/10.1103/PhysRevC.72.055502

[22] M. Sofo Haro, L. Arnaldi, et al, The data acquisition system of the Latin American Giant Observatory (LAGO), Nuclear Instruments and Methods in Physics Research Section A: Accelerators, Spectrometers, Detectors and Associated Equipment 820 (2016) 34 – 39. doi:https://doi.org/10.1016/j.nima.2016.02.101.

[23] A. Filevich, P. Bauleo, H. Bianchi, J. R. Martino, G. Torlasco, Spectral-directional reflectivity of Tyvek immersed in water, Nuclear Instruments and Methods in Physics Research Section A: Accelerators, Spectrometers, Detectors and Associated Equipment 423 (1) (1999) 108 – 118. doi:https://doi.org/10.1016/S0168-9002(98)01194-2.

[24] Hamamatsu, Permanent link to hamamatsu large photocathode area datasheet., Tech. rep. (2018).
URL https://www.hamamatsu.com/resources/pdf/etd/PMT_handbook_v3aE.pdf

[25] J. V. Jelley, Cherenkov radiation, and its applications, Pergamon Press, 1958.

[26] J. D. Jackson, Classical electrodynamics, 3rd Edition, Wiley, New York, NY, 1999.

[27] P. A. Cherenkov, Visible emission of clean liquids by action of gamma radiation., Doklady Akademii Nauk SSSR1 (1934) 451–462.

[28] P. A. Cherenkov, Visible radiation produced by electrons moving in a medium with velocities exceeding that of light., Physical Review (1937) 378–379.

Journal Pre-proof

[29] A. Etchegoyen, P. Bauleo, X. Bertou, C. Bonifazi, A. Filevich, M. Medina, D. Melo, A. Rovero, A. Supanitsky, A. Tamashiro, Muon-track studies in a water Cherenkov detector, Nuclear Instruments and Methods in Physics Research Section A: Accelerators, Spectrometers, Detectors and Associated Equipment 545 (3) (2005) 602 – 612. doi:https://doi.org/10.1016/j.nima.2005.02.016.

[30] S. F. Mughabghab, M. Divadeenam, N. E. Holden, Neutron Cross Sections, Vol. 1, Academic Press, 1981.

[31] R. B. Firestone, H. D. Choi, R. M. Lindstrom, et al, Database of Prompt Gamma Rays from Slow Neutron Capture for Elemental Analysis, Non-serial Publications, 2007.

[32] H. H. Li, Refractive index of alkali halides and its wavelength and temperature derivatives, Journal of Physical and Chemical Reference Data 5 (2) (1976) 329–528. doi:10.1063/1.555536.

[33] R. Khabaz, Assessment of gamma-rays generated by the spontaneous fission source ^{252}Cf using a Monte Carlo method, Annals of Nuclear Energy 46 (2012) 76–80.

[34] S. M. Seltzer, Calculation of photon mass energy-transfer and mass energy-absorption coefficients, Radiation Research 136 (1993) 147–170. doi:10.2307/3578607.
URL http://www.jstor.org/stable/3578607.

[35] O. Batenkov, A. Blinov, M. Blinov, S. Smirnov, Neutron emission from spontaneous-fission fragments, Soviet Atomic Energy (1988) 489–493doi:10.1007/BF01124588.

[36] J. W. Meadows, ^{252}Cf Fission Neutron Spectrum from 0.003 to 15.0 MeV, Physical Review (1967) 1076–1082doi:10.1103/PhysRev.157.1076.

[37] J. Allison, et al., Recent developments in Geant4.

Journal Pre-proof

[38] A. B. Smith, P. R. Fields, J. H. Roberts, Spontaneous Fission Neutron Spectrum of ^{252}Cf, Physical Review 108 (1957) 411–413. doi:10.1103/PhysRev.108.411.

[39] K. Beckurts, K. Wirtz., Neutron Physics, Springer Verlag, 1964.

[40] S. Dazeley, A. Bernstein, N. Bowden, R. Svoboda, Observation of neutrons with a Gadolinium doped water Cherenkov detector, Nuclear Instruments and Methods in Physics Research Section A: Accelerators, Spectrometers, Detectors and Associated Equipment 607 (3) (2009) 616 – 619. doi:https://doi.org/10.1016/j.nima.2009.03.256.

[41] S. Dazeley, A. Asghari, A. Bernstein, N. Bowden, V. Mozin, A water-based neutron detector as a well multiplicity counter, Nuclear Instruments and Methods in Physics Research Section A: Accelerators, Spectrometers, Detectors and Associated Equipment 771 (2015) 32 – 38. doi:https://doi.org/10.1016/j.nima.2014.10.028.

Journal Pre-proof

Declaration of interests

XX The authors declare that they have no known competing financial interests or personal relationships that could have appeared to influence the work reported in this paper.

☐The authors declare the following financial interests/personal relationships which may be considered as potential competing interests:

Journal Pre-proof